COMPUTERIZED BONE AGE ASSESSMENT FOR ZERO-TO-SEVEN AGE INTERVAL

by

İsmail Enes Özkalay

B.S., in Electronics Engineering, Istanbul Technical University, 2006

Submitted to the Institute of Biomedical Engineering
in partial fulfillment of the requirements
for the degree of
Master of Science
in
Biomedical Engineering

Boğaziçi University
2010

ACKNOWLEDGMENTS

I would like to thank to my thesis supervisor Assoc. Prof. Dr. Albert Güveniş for his valuable support and motivation during this master thesis study. Also, I would like to thank to Image Processing and Informatics Lab of University of Southern California for providing the hand x-ray images used in this study.

Additionally, I would like to thank to all of my friends from Biomedical Engineering Institute in Bogazici University for their friendship and helpful contribution during my study. Especially I want to mention the names of Ömer Sağli, Didar Talat, and Bora Büyüksaraç for sharing their valuable ideas.

I can not forget the support of my family not only for this thesis study but also over the entire course of my life.

Finally, I would like to thank to Prof. Dr. Mehmet Özkan for providing me his laboratory, so giving me the chance to have such a nice environment to pursue my studies.

ABSTRACT

COMPUTERIZED BONE AGE ASSESSMENT FOR ZERO-TO-SEVEN AGE INTERVAL

The goal of this thesis is to study the use of neural networks for radiological bone age assessment from hand and wrist x-ray images is done. Carpal bones have been considered for bone age assessment. While the both semi-automatically and manually marked carpal bone features are given to our system as inputs, bone age is produced as an output. Additionally, chronological age, radiologist readings and sex information are used besides carpal bones and finally, the results are investigated. In this study, real data sets have been used. This study is important because a very simple and efficient method by using all 7 carpal bones is developed for assessing the bone age of children instead of the complicated methods in the literature. This semi-automated method also improves the time efficiency compared to the widely used manual methods such as GP, TW2. Inclusion of carpal bones for assessing bone age of children is mandatory. However, due to various factors including the uncertain number of bones appearing, non-uniformity of soft tissue, low contrast between the bony structure and soft tissue, automatic segmentation and identification of carpal bone boundaries is a hard endeavor. In this study, semi-automated carpal bone segmentation and age assessment software is developed and implemented. Also, neural network classification is used to assess the bone age depending on the selected features from carpal bones. In our application, 236 training images and 58 test images are used for 0 to 7 age group. After application, it is illustrated that results are considerably comparable with both chronological bone age and the two radiologist readings. We therefore conclude that the developed system may replace the manual methods for improved speed and comparable accuracy.

Keywords: Computerized bone age assessment, Greulich and Pyle (GP) method, Tanner and Whitehouse method, neural network, carpal bone

ÖZET

0-7 YAŞ ARASI İÇİN BİLGİSAYARLI KEMİK YAŞI TESPİTİ

Bu tezin amacı, el ve bilek X-ray görüntülerinden sinir ağları kullanımıyla radyolojik kemik yaşı değerlendirmesi yapmaktır. Kemik yaşı tespiti için karpal kemikler kullanılmaktadr. Yarı otomatik ve manuel olarak belirlenen karpal kemik özellikleri otomatik sisteme girdi olarak verilirken, bilgisayarlı kemik yaşı çıkış olarak alınır. Ayrıca, kronolojik yaş, radyolog değerleri ve cinsiyet bilgileri de karpal kemiklere ek olarak kullanılmış ve sonuçlar incelenmiştir. Bu çalışmada gerçek veri setleri kullanılmış olup, literatürdeki karmaşık yöntemlere kıyasla, yedi karpal kemik kullanılarak çok basit ve etkili bir yöntem geliştirilmiştir. Bu yarı otomatik yöntem çokça kullanılan GP ve TW2 yöntemlerine kıyasla zaman açısından avantajlıdır. Çocukların kemik yaşı değerlendirmesinde karpal kemiklerin dahil edilmesi zorunludur. Bununla beraber, belirsiz sayıda kemik gözükmesi, yumuşak dokunun değişken olması, kemik yapısı ve yumuşak doku arasındaki düşük kontrast, karpal kemik sınırlarının otomatik segmentasyonu ve belirlenmesi gibi faktörlerden ötürü gerçekten zor bir iştir. Bu çalışmada, yarı otomatik karpal kemik segmentasyonu ve yaş tespiti için bilgi temelli bir yöntem geliştirildi ve uygulandı. Ardından, karpal kemik özelliklerine bağlı olarak sinir ağları uygulamasıyla kemik yaşı tespit edilmiştir. Uygulamada 236 Xray görüntüsü eğitim amaçlı, 58 görüntü ise test amaçlı kullanılmıştır. Uygulamanın sonunda, yarı otomatik sistem ile elde edilen sonuçların kronolojik yaş ve iki radyoloğun okumalarıyla karşılaştırılabilir olduğu sonucu elde edilmiştir. Sonuç olarak, geliştirdiğimiz sistem manuel yöntemlerin yerini gelişmiş hız ve benzer doğruluk oranlarıyla alabilir.

Anahtar Sözcükler: Bilgisayarlı kemik yaşı analizi, Greulich and Pyle (GP) methodu, Tanner and Whitehouse methodu, sinir ağları, karpal kemik.

TABLE OF CONTENTS

LIST OF FIGURES

LIST OF TABLES

LIST OF ABBREVIATIONS

GP	Greulich and Pyle
TW2	Tanner and Whitehouse 2
ROI	Region of Interest
HIS	Hispanic
BAA	Bone Age Assessment
USA	United States of America
EMROI	Epiphyseal Metaphyseal Region of Interest
RUS	Radius, Ulna, and Short finger bones
PROI	Phalangeal Region of Interest
CR	Computed Radiography
LAMF	Longitudinal axis of the middle finger
CROI	Carpal Region of Interest
GUI	Graphical User Interface
Cap.	Capitate
Ham.	Hamate
Triq.	Triquetral
Lun.	Lunate
Scap.	Scaphoid

1. INTRODUCTION

1.1 Objective And Motivation

The determination of skeletal maturity has a very important role in diagnostic and therapeutic investigations of endocrinological problems and also growth disorders of children. Conventional approach of bone age assessment (BAA) is both a time consuming procedure and depends on the physician. The aim of this thesis is to improve the efficiency and objectivity of BAA process.

1.2 Uses of Skeletal Bone Age Assessment

Assessment of skeletal age is helpful in the monitoring of growth hormone therapy and diagnosis of endocrine disorders. The incongruity between the skeletal age and the chronological age may indicate abnormalities in the bone ossification. Delayed or accelerated appearance of ossification centers caused by an illness may serve as an example [1].

Bone Age Assessment is also performed when surgery for correcting deformities of the long bones or the vertebral column is planned. Bone age determinations are also commonly used to predict individual's final height.

The classical method of skeletal bone age assessment (BAA) utilizes the recognition of changes in the radiographic appearance of the maturity indicators in a hand-wrist radiograph by comparison with a reference data set which consists of series of radiographs grouped according to sex and age. The most commonly used reference standard is the atlas published by Greulich and Pyle (GP) [2]. They were derived from the population of the middle socioeconomic class of Caucasian children from Midwest, USA from 1931 to 1942. The atlas remains unchanged from its initial publication and is

commonly used in clinical practice to assess bone age of children of Caucasian, African-American, Hispanic, Asian, and other descent. The examination is subjective because the radiologist analyzes each individual bone of the hand and wrist, determines an overall bone age, and finally fits the amalgamated results into a closest match to the reference radiographs in the atlas.

2. BONE AGE ASSESSMENT METHODS

2.1 Introduction

Bone age assessment is frequently performed in pediatric patients to evaluate growth and to diagnose and manage a multitude of endocrine disorders and pediatric syndromes. For decades, the determination of bone maturity has relied on a visual evaluation of the skeletal development of the hand and wrist, most commonly using the Greulich and Pyle atlas.With the advent of digital imaging, multiple attempts have been made to develop image-processing techniques that automatically extract the key morphological features of ossification in the bones to provide a more effective and objective approach to skeletal maturity assessments. However, the design of computer algorithms capable of automatically rendering bone age has been impeded by the complexity of evaluating the wide variations in bone mineralization tempo, shape and size encompassed in the large number of ossification centers in the hand and wrist. Clearly, developing an accurate digital reference that integrates the quantitative morphological traits associated with the different degrees of skeletal maturation of 21 tubular bones in the hand and 7 carpal bones in the wrist is not an easy task [3].

2.2 Bone Development

2.2.1 Growth Pattern of Carpal Bones

At the early stage of development, carpals appear as dense pin points on a radiograph. During development, they increase in size until reaching their optimal sizes and characteristic shapes. Figure 2.1 shows an ROI image with seven carpal bones appearing.

Figure 2.2 demonstrates the growth pattern of carpal bones of Asian males

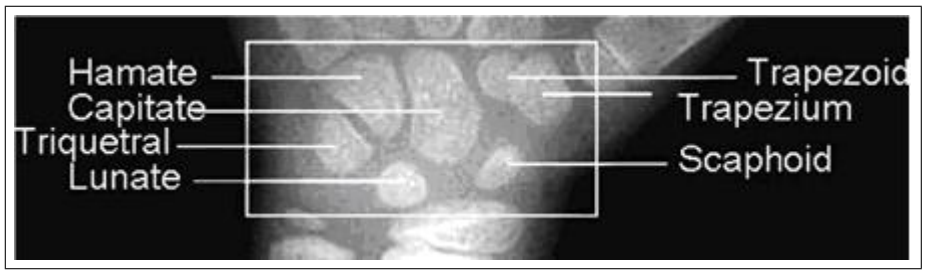

Figure 2.1 Description of carpal bones in a hand radiograph

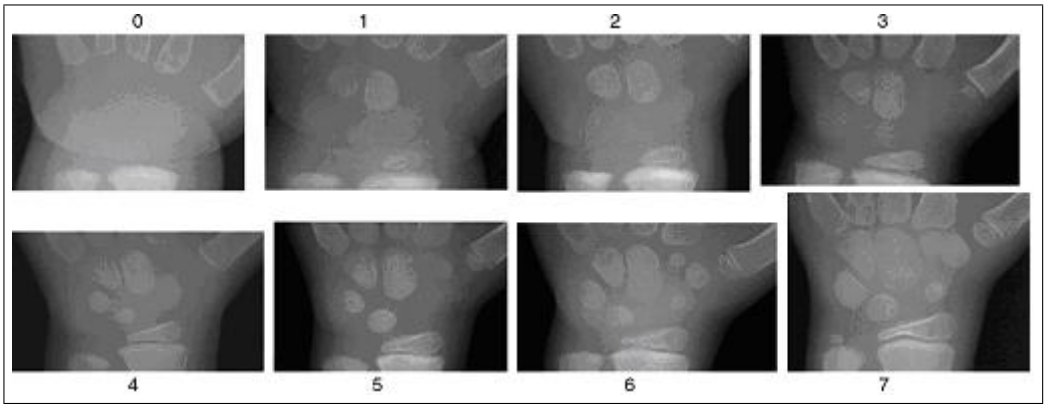

Figure 2.2 Growth pattern of carpal bones of Asian male from newborn to 7-year-old

from newborn to 7-year-old. Carpal bones ossified in chronological order, Capitate, Hamate, Triquetral, Lunate, followed usually by Scaphoid, then either the Trapezium or the Trapezoid [4] [5]. Female developments noticeably more advanced than male by as many as 3 years.

Medical study [6] indicated that, due to the nature of carpal bone maturity, their analysis does not provide accurate and significant information for patients older than 7-12 years of age. This is due to the fact that carpal bones start overlap at age around 7-year-old in male and 5 in female. In this stage of development the phalangeal analysis yields more reliable information. Therefore, in this research, carpal bone analysis focuses on age group from 0 to 7 for male and 0 to 5 for female. The reason for that is also explained in Table 2.1.

Table 2.1
Reliability of ROI analysis for different age groups in CAD method

	ROI	
Age Group (years)	Phalangeal ROI analysis	Carpal ROI analysis
0-5(female), 0-7(male)	Size and shape analysis of epimetaphysis feature extraction is not reliable	Size and shape analysis of carpal bones feature extraction is reliable
6-12(female), 8-12(male)	Size and shape analysis of epimetaphysis feature extraction is reliable	Degree of overlapping of carpal bones feature extraction is not reliable
13-18(female and male)	Degree of fusion of epimetaphysis feature extraction is reliable	

2.2.2 Growth Pattern of Long Bones

Skeletal maturity is a measure of development incorporating the size, shape and degree of mineralization of bone to define its proximity to full maturity. The assessment of skeletal maturity involves a rigorous examination of multiple factors and a fundamental knowledge of the various processes by which bone develops. Longitudinal growth in the long bones of the extremities occurs through the process of endochondral ossification. In contrast, the width of the bones increases by development of skeletal tissue directly from fibrous membrane. The latter is the mechanism by which ossification of the caldarium, the flat bones of the pelvis, the scapulae, and the body of the mandible occurs. Initial calcification begins near the center of the shaft of long bones in a region called the primary ossification center [7].

Although many flat bones, including the carpal bones, ossify entirely from this

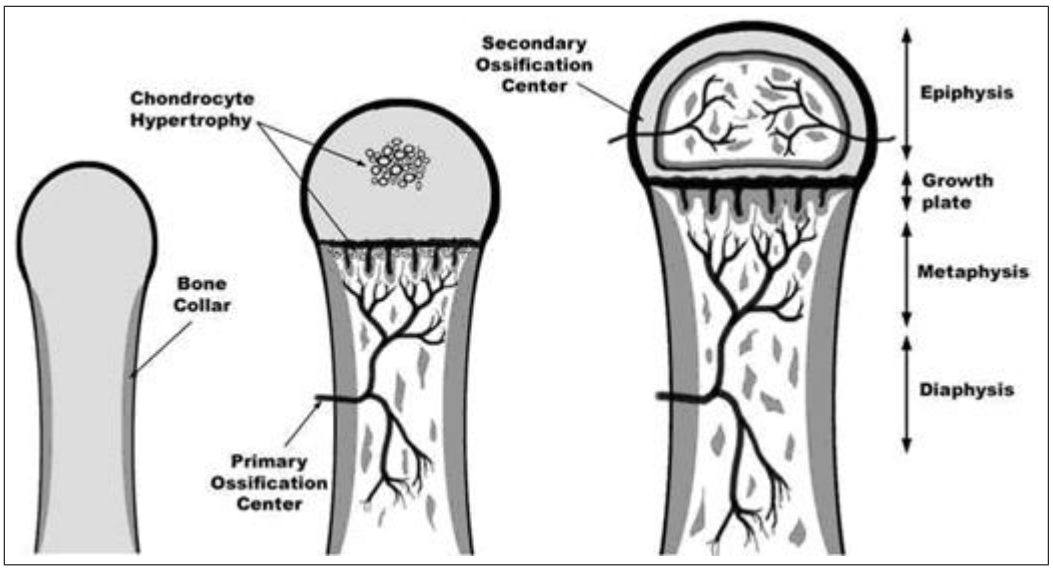

Figure 2.3 Schematic representation of endochondral bone formation

primary center, all of the long bones develop secondary centers that appear in the cartilage of the extremities of the bone. Maturation in these centers proceeds in a manner identical to that in the primary centers with ossification of cartilage and invasion of osteoclasts and osteoblasts [3].

The bone ossified from the primary center is the diaphysis, while the bone ossified from the secondary center is the epiphysis. As the secondary center is progressively ossified, the cartilage is replaced by bone until only a thin layer of cartilage, the epiphyseal plate, separates the diaphyseal bone from the epiphysis. The part of the diaphysis that abuts on the epiphysis is referred to as the metaphysis and represents the growing end of the bone. As long as the epiphyseal cartilage plate persists, both the diaphysis and epiphysis continue to grow, but, eventually, the osteoblasts cease to multiply and the epiphyseal plate is ossified. At that time, the osseous structures of the diaphysis and epiphysis are fused and growth ceases [7].

In the fetal phase of life, the principle interest in skeletal growth is associated with the diagnosis of prematurity. The end of the embryonic period and the beginning of the fetus is marked by the event of calcification, which begins at 8 or 9 weeks. By the 13th fetal week, most primary centers of the tubular bones are well-developed

into diaphyses, and, at birth, all diaphyses are completely ossified, while most of the epiphyses are still cartilaginous. Ossification of the distal femoral epiphysis begins during the last two months of gestation, and this secondary center is present in most full term babies. Similarly, the ossification center for the proximal epiphysis of the humerus usually appears about the 40th week of gestation. On the other hand, the centers for the proximal epiphyses of the femur and tibia may not be present in full term infants, but appear in the first few months of life [8][9]. After birth, the epiphyses gradually ossify in a largely predictable order, and, at skeletal maturity, fuse with the main body of the bone. Comparing the degree of maturation of the epiphyses to normal age-related standards forms the basis for the assessment of skeletal maturity, the measure of which is commonly called bone age or skeletal age. It is not clear which factors determine a normal maturational pattern, but it is certain that genetics, environmental factors, and hormones, such as thyroxine, growth hormone, and sex steroids, play important roles. Studies in patients with mutations of the gene for the estrogen receptor or for aromatase enzyme have demonstrated that it is estrogen that is primarily responsible for ultimate epiphyseal fusion, although it seems unlikely that estrogen alone is responsible for all skeletal maturation [10].

2.2.3 Clinical Applications for Skeletal Determinations

A single reading of skeletal age informs the clinician of the relative maturity of a patient at a particular time in his or her life, and, integrated with other clinical findings, separates the normal from the relatively advanced or retarded. Successive skeletal age readings indicate the direction of the child's development and/or show his or her progress under treatment. In normal subjects, bone age should be roughly within 10 percent of the chronological age. Greater discordance between skeletal age and chronological age occurs in children who are obese or who start puberty early, as their skeletal age is accelerated [3].

There are two main applications for evaluations of skeletal maturation: the diagnosis of growth disorders and the prediction of final adult height.

2.2.4 Diagnosis of Growth Disorders

Assessments of skeletal age are of great importance for the diagnosis of growth disorders, which may be classified into two broad categories with different etiologies, prognoses and treatments. Primary growth deficiency is due to an intrinsic defect in the skeletal system, such as bone dysplasia, resulting from either a genetic defect or prenatal damage and leading to shortening of the diaphysis without significant delay of epiphyseal maturation.

Hence, in this form of growth disorder, the potential normal bone growth and therefore, body growth are impaired, while skeletal age is not delayed or is delayed much less than is height [3].

Secondary growth deficiency is related to factors, generally outside the skeletal system, that impair epiphyseal or osseous maturation. These factors may be nutritional, metabolic, or unknown, as in the syndrome of idiopathic (constitutional) growth delay. In this form of growth retardation, skeletal age and height may be delayed to nearly the same degree, but, with treatment, the potential exists for reaching normal adult height.

The distinction between these categories may be difficult in some instances in which skeletal age is delayed to a lesser degree than height. In general, however, differentiation between primary and secondary categories of growth failure can be determined from clinical findings and skeletal age [11].

2.2.5 Conventional Techniques for Skeletal Determinations

In the evaluation of physical development in children, variations in maturation rate are poorly described by chronological age. Thus, for many decades, scientists have sought better techniques to assess the degree of development from birth to full maturity. Measures of height, weight, and body mass, although closely related to bi-

ological maturation, are not sufficiently accurate due to the wide variations in body size. Similarly, the large variations in dental development have prevented the use of dental age as an overall measure of maturation, and other clinically established techniques are of limited value. As examples, the age atmenarche, although an important biological indicator, relates to only half the population, and determinations of sexual development using the Tanner classification, while an extremely useful clinical tool, is subjective and restricted to the adolescent period [3].

Unfortunately, most available maturational age scales have specific uses and tempos that do not necessarily coincide. Skeletal age, or bone age, the most common measure for biological maturation of the growing human, derives from the examination of successive stages of skeletal development, as viewed in hand-wrist radiographs. This technique, used by pediatricians, orthopedic surgeons, physical anthropologists and all those interested in the study of human growth, is currently the only available indicator of development that spans the entire growth period, from birth to maturity. Essentially, the degree of skeletal maturity depends on two features: growth of the area undergoing ossification, and deposition of calcium in that area. While these two traits may not keep pace with each other, nor are they always present concurrently, they follow a fairly definite pattern and time schedule, from infancy to adulthood. Through radiographs, this process provides a valuable criterion for estimating normal and abnormal growth and maturation [3].

Greulich and Pyle and Tanner-Whitehouse (TW2) are the most prevalently employed skeletal age techniques today [2][12]. Despite their differing theoretical approaches, both are based on the recognition of maturity indicators, i.e., changes in the radiographic appearance of the epiphyses of tubular bones from the earliest stages of ossification until fusion with the diaphysis, or changes in flat bones until attainment of adult shape [13].

The standards established by Greulich and Pyle, undoubtedly the most popular method, consist of two series of standard plates obtained from hand-wrist radiographs of white, upper middle-class boys and girls enrolled in the Brush Foundation Growth

Study from 1931 to 1942. Represented in the Greulich and Pyle atlas are 'central tendencies', which are modal levels of maturity within chronological age groups. The skeletal age assigned to each standard corresponds to the age of the children on whom the standard was based. When using the Greulich and Pyle method, the radiograph to be assessed is compared with the series of standard plates, and the age given to the standard plate that fits most closely is assigned as the skeletal age of the child. It is often convenient to interpolate between two standards to assign a suitable age to a radiograph. The apparent simplicity and speed with which a skeletal age can be assigned has made this atlas the most commonly used standard of reference for skeletal maturation worldwide [3].

Underlying the construction of the Greulich and Pyle atlas are the assumptions that, in healthy children, skeletal maturation is uniform, that all bones have an identical skeletal age, and that the appearance and subsequent development of body centers follow a fixed pattern. However, considerable evidence suggests that a wide range of normal variation exists in the pattern of ossification of the different bones of the hand and the wrist and that this variation is genetically determined. In fact, most standards in the atlas include bones that differ considerably in their levels of maturity [2].

Greulich and Pyle did not formally recommend any specific technique for the use of their atlas. Rather, they suggested that atlas users develop their own method depending on their preferences. Pyle et al did, however, suggest the rather cumbersome approach that each ossification center be assigned a bone-specific bone age, and the average of the ages calculated. By and large, when there is a discrepancy between the carpal bones and the distal centers, greater weight should be assigned to the distal centers because they tend to correlate better with growth potential [11].

A number of important caveats concerning bone age must be considered. First, experience in skeletal maturity determinations and a similar analytic approach are essential to enhance inter- and intra-observer reproducibility. Clinical studies and trials involving bone age as an outcome measure greatly benefit from the inclusion of experienced readers who use similar approaches in their assessments. Second, the normal

rate of skeletal maturation differs between males and females, and ethnic variability exists. Lastly, these references are not necessarily applicable to children with skeletal dysplasias, endocrine abnormalities or a variety of other causes of growth retardation [3].

2.2.6 Computer Assisted Techniques for Skeletal Determinations

With the advent of digital imaging, several investigators have attempted to provide an objective computer-assisted measure for bone age determinations and have developed image processing techniques from reference databases of normal children that automatically extract key features of hand radiographs [14] [15]. To date, however, attempts to develop automated image analysis techniques capable of extracting quantitative measures of the morphological traits depicting skeletal maturity have been hindered by the inability to account for the great variability in development and ossification of the multiple bones in the hand and wrist. In an attempt to overcome these difficulties, automated techniques are being developed that primarily rely on measures of a few ossification centers, such as those of the epiphyses [3].

In the design of this computerized bone age assessment system, the complexities associated with the design of software that integrates all morphological parameters were circumvented through the selection of an alternative approach. Artificial, idealized, sex- and age-specific images of skeletal development that incorporated the different degrees of maturation of each ossification center in the hand and wrist is designed. The neural network which evaluates the test images and come up with the bone age output is derived from a composite of several hand radiographs from healthy children that are identified as the perfect average for each ossification center in zero-to-seven age group [3].

2.2.7 Methods of Bone Age Assessment in Practice

Greulich and Pyle method (GP) and Tanner and Whitehouse (TW2) use atlas matching methods for manual determination of skeletal age. GP method is easier and faster to use compare to TW2 method. However TW2 method is more reliable.

Both methods rely on radiographs taken from the left hand. Prior to detailed examination of the two methods it is useful to know a little about the anatomy of the hand in order to understand some of the terms used. Figure 2.4 and Figure 2.5 show the most important bones for skeletal age determination in the hand. In Figure 2.4 we see a schematic representation of the bones of the hand. Figure 2.5 shows an actual hand radiograph. The most important hand bones are those of the fingers, the proximal, middle and distal phalanges. The thumb has only proximal and distal phalanges. Next there are the carpal bones, Capitate, Hamate, Triquetral, Lunate, Scaphoid, Trapezium and Trapezoid. In the middle we see the five metacarpals.

Ossification centers are located between the phalanges of developing children. Because the radiograph in Figure 2.5 is of an adult subject they can not be seen. In Figure 2.6 an example of the situation in the developing children so it can be seen. We can clearly see three parts, the metaphysis, the epiphysis and the diaphysis. We call that structure as an Epiphyseal-Metaphyseal Region of Interest (EMROI). This structure changes during the development of the skeleton. The epiphysis becomes steadily wider and eventually fuses with the metaphysis.

2.2.7.1 The Greulich and Pyle Method. First studies on the human growth and development started in 1929 at the Western Reverse University School of Medicine in Ohio. A Large number of children of different ages were used in these studies. Left shoulder, elbow, hand, hip and knee radiographs were taken for examination. In the first postnatal year an examination was conducted every three months, from twelve months to five years they were examined each 6 months and annually thereafter. In total the study ran from 1931 until 1942. In 1937 "Atlas of Skeletal Maturation of

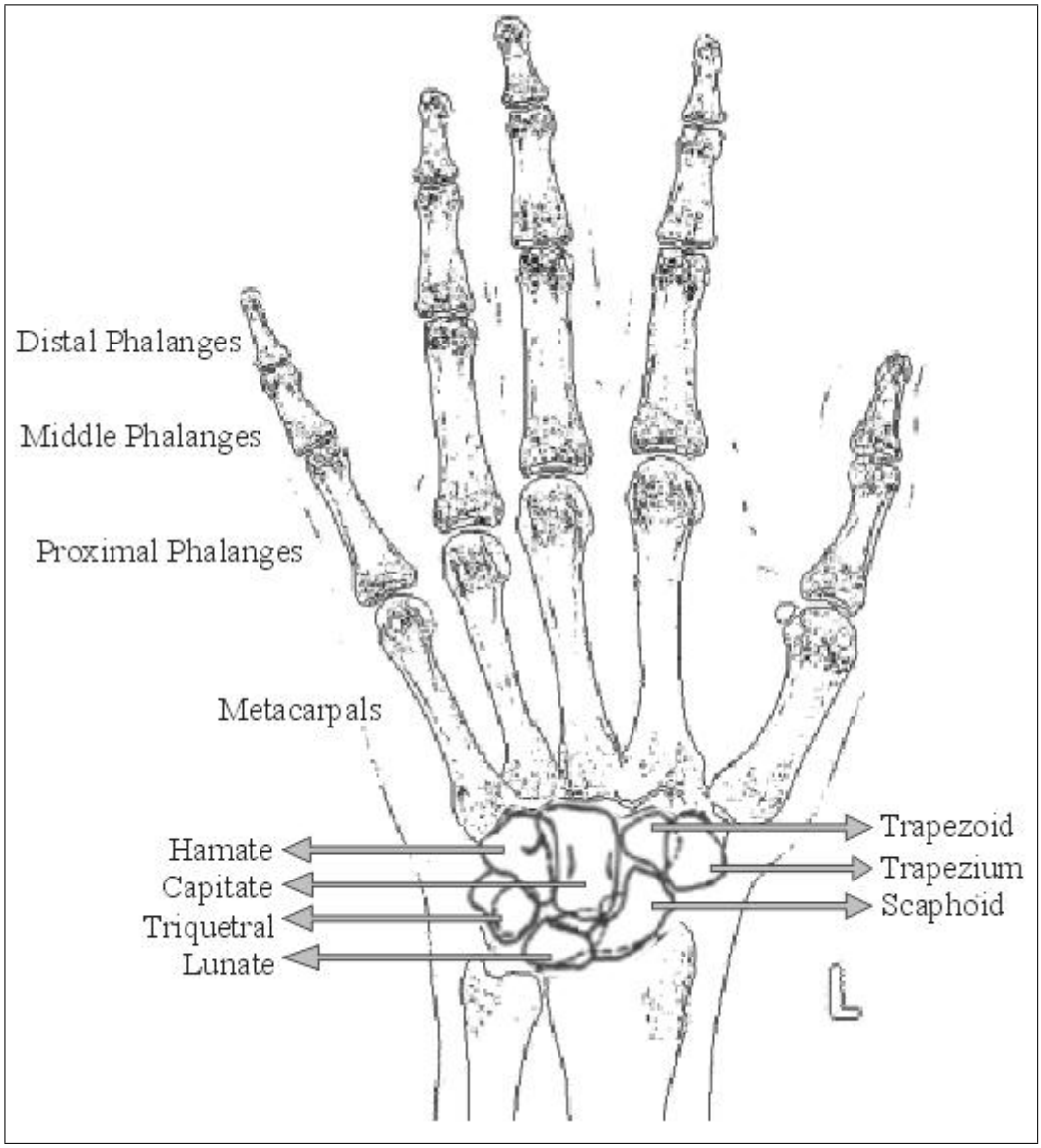

Figure 2.4 Anatomy of left hand

Figure 2.5 Radiograph of Left Hand

Hand" was published by Todd [16].

The Greulich-Pyle has been used extensively by orthopedists and was used by Green and Anderson in compiling their data for growth remaining in children nearing skeletal maturity. Since the Moseley straight line graph was based on the Green-Anderson data, the Greulich-Pyle system is correlated with that graph also. The two methods do not give equivalent bone ages. The Tanner-Whitehouse with computer assistance may be more reproducible, but it is more cumbersome to use. For the present, the Greulich-Pyle method is still standard for the orthopedic use, even though it was derived more than a half century ago on an exclusively white upper-middle class population.

Assessment steps:

1. Assess one bone at a time
2. Locate the atlas plate that most closely resembles the X-Ray bone
3. Interpolate between atlas plates
4. Assess a second time
5. Average the two twenty-eight assessments

In the Greulich and Pyle method twenty-eight bones are compared against the reference atlas. All the bones in the hand and wrist are examined and average of the assessments gives us the bone age of patient.

Development stages of each bone are described in the atlas in Figure 2.7. The descriptions in the figure are more a general guideline to the development of each bone in the hand rather than an instruction on how to rate a bone. Most institutions are using a more rapid modified version of the original atlas, which is also potentially less accurate. This version is described below.

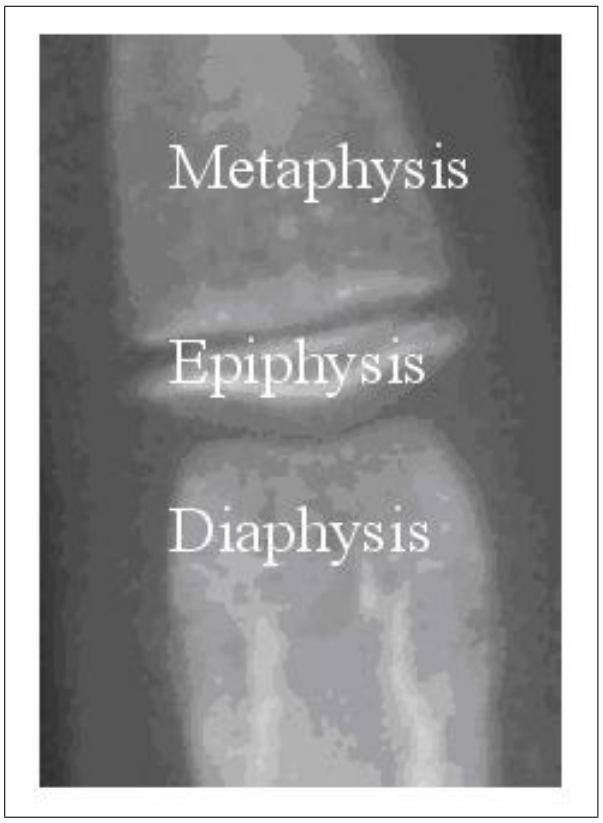

Figure 2.6 The ossification centers on finger

The atlas is divided into two parts, one for the male patients and one for the female patients because females develop quicker than males. Each part contains standard radiographic images of the left hand of children ordered by the chronological age.

To measure skeletal age of a patient first of all, the radiograph of the patient is compared with the image in the atlas that is match with the chronological age of the patient. Next, one should compare it with the adjacent images representing both younger and older children. There are some maturity indicators when comparing the radiograph of the patient against an image in the atlas. These features can vary with the race, age and sex of the child. In the younger children the presence or absence of the certain carpal or epiphyseal ossification centers are often pointers for the physician about the skeletal age of a child. In older children the shape of the epiphyses and the amount of fusion with the metaphysis is a good indicator for the skeletal age, carpal ossification centers did not differ at that time. Once the atlas image that most resembles the radiograph is found, the physician should conduct a more detailed examination of

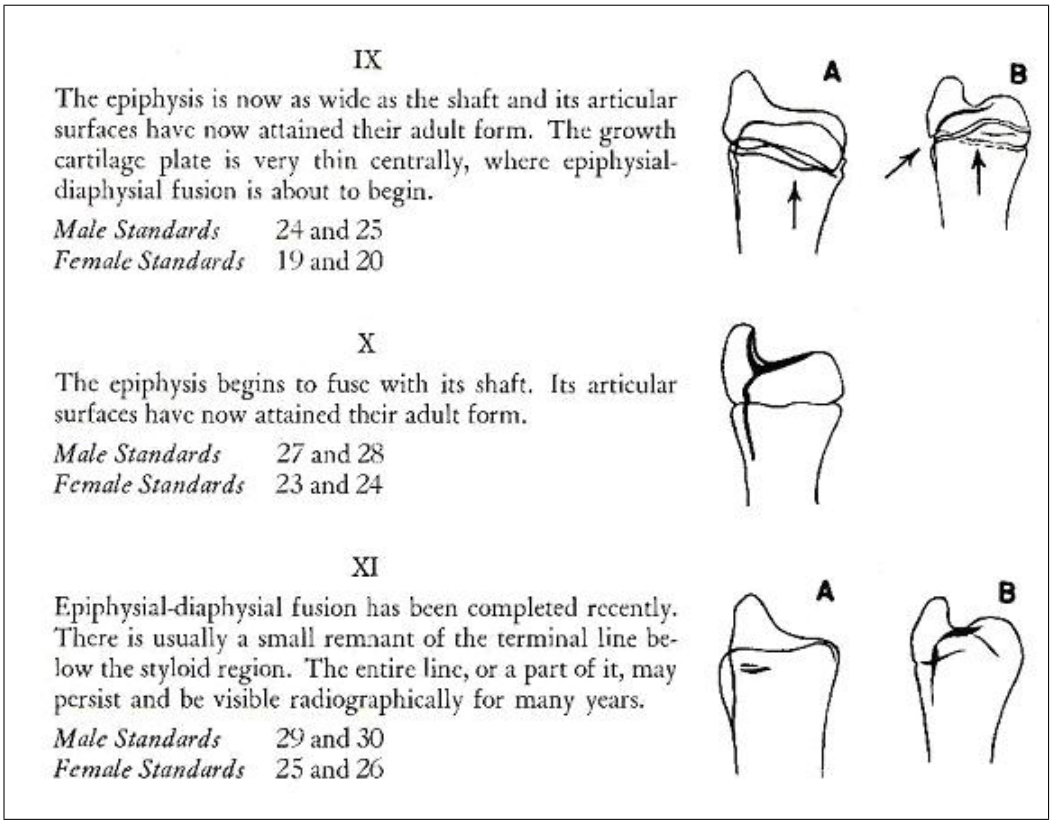

Figure 2.7 Descriptions of the skeletal development found in the Greulich and Pyle atlas

the individual bones and epiphyses. So we can find the skeletal age when the matching radiograph has been found.

2.2.7.2 The Tanner and Whitehouse (TW2) Method. Tanner and Whitehouse knew about the Greulich and Pyle atlas and the way in which it was used. They noticed several aspects of the method that they felt needed to be improved. According to them the subjectivity of the matching process was an obvious weakness of the GP method. Physicians generally look at the whole radiograph at once and then compare it with an image in the atlas. Often a specific radiograph does not match any of the images in the atlas exactly, and little guidance is given on how to balance out the discrepancies that arise from one bone being more or less advanced than its match in the atlas.

The scale used for expressing the maturity was another aspect of the GP method TW2 didn't like. Each standard radiograph in the atlas has the age of the child from whom it was taken associated with it. Therefore maturity is measured on an age scale. It could even be seen as the predicted age, because the matching process gives the most likely chronological age of the child being matched, as judged from the radiograph. This most likely age is then said to be the skeletal age. Tanner and Whitehouse deemed that a new, more sophisticated system was needed which would not make use of an age scale for maturity measurements. In their view a maturity scale should be defined in a manner which does not directly relate to age. This would allow them to produce a set of "maturity standards" of any given population by studying the relationship between maturity and age.

To build standard atlas radiographs of up to 12 years old, healthy children were used in the period of six mounts. Changes in the shape and density markings of each bone were recorded in standard atlas. After this the different stages were identified, these stages had to be universally present in all individuals.

Features that were only present in the bones of particular subjects were excluded,

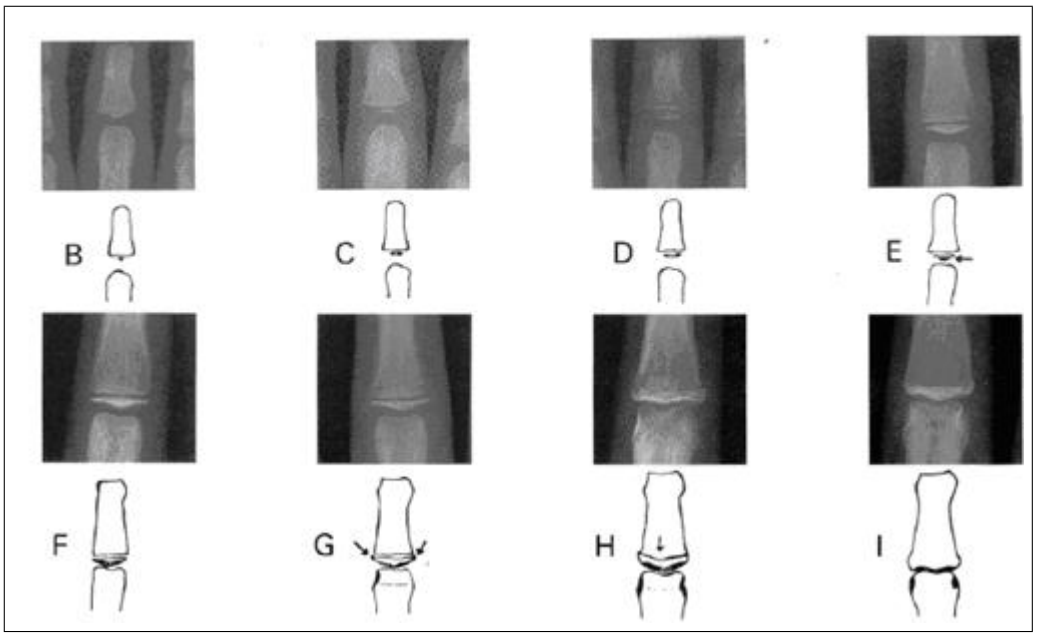

Figure 2.8 Stages of middle phalanx of the third finger in the hand

also absolute size was always ignored. The exact number of stages for each bone was chosen so that differences between consecutive stages were neither so small as to cause confusion and rating error, nor so large that significant information was lost.

A score had to be assigned to each bone in the hand for each stage. Many of the bones in the hand and wrist are giving approximately the same information about maturity. This is especially true for the bones in the fingers. Therefore it is not desirable to just take an average of all the scores in a hand since this would give the nineteen finger bones together a much greater importance than the seven carpals or the radius and the ulna. A system of weighted scores was developed in order to correct for this. Also, the scores of boys and girls are different because girls mature faster than boys. Especially in older children the carpal bones do not provide any useful information about the skeletal maturity. To allow the exclusion of the carpals or the specific examination of them, three separate scoring systems were developed:

- TW2 20-bone
- RUS

- Carpal

The first system is the most extensive one featuring 20 bones of the hand. These bones include bones of the wrist, the carpal bones, and bones of the thumb and the third and fifth fingers. The second system named RUS (Radius, Ulna and Short finger bones) contains the same bones as the first one except for the carpals. Finally the third system contains only the carpal bones. Using the TW2 method is relatively straightforward; first one chooses a suitable scoring system (TW2, RUS or carpal). A suitable scoring system is mostly determined by the calendar age of the patient.

Next one looks up the bones in the radiograph that are associated with that particular system. Those particular bones are then compared to a series (see Figure 2.8) of reference images in the TW2 book. These reference images each represent one developmental stage (B-I) and are backed up by textual descriptions. In these descriptions of a stage, important changes in the bones are described. Also, the descriptions often contain requirements that a bone must meet in order to be classified a certain stage.

The reference image that most resembles the bone from the radiograph is chosen. Of course the bone must also meet the requirements in the description. The stage corresponding to a reference image is assigned to the bone. When the stage of a certain bone is known the score associated with that particular bone and stage can be looked up. After all the required bones have been analyzed and all the needed scores have been gathered, the total score is determined by adding all the separate scores.

3. PREVIOUS WORK ABOUT AUTOMATED BONE AGE ASSESSMENT

3.1 State of the Art

3.1.1 Carpal Bone Oriented

An automatic computer-aided-diagnosis (CAD) method has been previously developed based on features extracted from phalangeal regions of interest (ROI) in a digital hand atlas, which can assess bone age of children from ages 7 to 18 accurately around 2007 by Zhang[17]. Zhang illustrated in his study that in order to assess the bone age of children in younger ages, the inclusion of carpal bones is necessary. However, due to various factors including the uncertain number of bones appearing, non-uniformity of soft tissue, low contrast between the bony structure and soft tissue, automatic segmentation and identification of carpal bone boundaries is an extremely challenging task. In this study, author developed and implemented a knowledge-based method for fully automatic carpal bone segmentation and morphological feature analysis. Fuzzy classification was then used to assess the bone age based on the selected features. This method has been successfully applied on all cases in which carpal bones have not overlapped. CAD results of total about 205 cases from the digital hand atlas were evaluated against subject chronological age as well as readings of two radiologists. Finally, it was found that the carpal ROI provides reliable information in determining the bone age for young children from newborn to 7-year-old.

Hsieh [18] proposed that automatic bone age estimation system was based on the phalanx geometric characteristics and carpals fuzzy information.The system could do automatic calibration by analyzing the geometric properties of hand images. Physiological and morphological features are extracted from medius image in segmentation stage. Back-propagation, radial basis function, and support vector machine neural networks were applied to classify the phalanx bone age. In addition, the proposed fuzzy

bone age (BA) assessment was based on normalized bone area ratio of carpals. The result reveals that the carpal features can effectively reduce classification errors when age is less than 9 years old. Meanwhile, carpal features will become less influential to assess BA when children grow up to 10 years old. On the other hand, phalanx features become the significant parameters to depict the bone maturity from 10 years old to adult stage. Owing to these properties, the proposed novel BA assessment system combined the phalanxes and carpals assessment. Furthermore, the system adopted not only neural network classifiers but fuzzy bone age confinement and got a result nearly to be practical clinically.

Around 1993 Pietka [19] developed image processing techniques for hand-bone analysis with using a digital radiograph to assess skeletal age. It consists of two steps, phalangeal and carpal bone analysis. This paper presents the carpal bone analysis. First, the carpal bone region of interest (CROI) is defined using a standard thresholding technique to separate the hand from the background. Then, a dynamic thresholding method with variable window sizes is used to differentiate between the bones from the soft tissue. Next, the radius, ulna and metacarpals intersecting the borders of the CROI are removed by using mathematical morphology. Finally, all objects included in the corrected CROI are separated and described in terms of features. These features describe the size, shape, and location. They also include some gray scale pixel value information. On the basis of this analysis the separation of the noncarpal bone objects from the carpal bones is possible. Feature selection step removes features of low discriminant power and reduces the space dimension. The remained carpal bone parameters are used for further analysis leading to the skeletal age assessment.

In 2004 Lin developed a system for the features analysis of the carpal bones which can reveal the important information for skeletal age assessment. The work faces the problem of the detection of carpal-bone features from its radio-image. A novel and effective segmentation technique is presented in this work with carpal bone image for skeletal age estimation. Carpal bone segmentation is a critical operation of the automatic skeletal age assessment system. This method consists of three procedures. First, the original carpal bone image is preprocessed via anisotropic diffusion. Then,

the carpal bone image is segmented by GVF-Snake model. Third, experiments are carried out on images of carpal bone. The results are very promising. In particular the method is able to extract overlapping carpal bones.

Liu [20] worked on the new algorithms to improve the validity, accuracy and practicality of automatic bone age assessment (ABAA). In this study, concept of object-based region of interest (ROI) was proposed. Thirteen RUS (including radius, ulna and short finger bones) ROIs and seven carpal ROIs were appointed respectively according to Tanner-Whitehouse (TW3) method. Five features including size, morphologic features and fusional/adjacent stage of each ROI were extracted based on particle swarm optimization (PSO) and input into ANN classifiers. ANNs were built upon feed-forward multi layer networks and trained with back-propagation algorithm rules to process RUS and carpal features respectively. About 1046 digital left hand-wrist radiographs were randomly utilized half for training ANNs and the rest for ABAA after manual reading by TW3 method. Thus, PSO method made image segmentation and feature extraction more valid and accurate, and the ANN models were sophisticated in processing image information. ABAA system based on intelligent algorithms had been successfully applied to all cases from 0 to 18 years of bone age.

3.1.2 Phalangeal Region of Interest Oriented

Previous studies will be discussed in this chapter. There are two parts in this chapter; first part on segmentation. The second is on assigning TW2 stages to ROIs.

A semi automatic bone age assessment system was developed by Micheal [21] around 1989, this system was named HANDX. The author claims that the system was able to automatically segment the bones in a hand radiograph but large scale tests were not done. Firstly preprocessing steps applied to images to normalize the image gray scale so that the later segmentation step will be more robust. The program first segments the entire hand from the background using a threshold operation. After this a model-based method is used to find the bones in the hand. This method uses

knowledge of the relative positions of the bones in the hand with respect to each other and to the contour of the hand to find the approximate position of a bone. Then its contour is given by an adaptive contour.

Another method developed by Pietka [22] is about to find the third finger and measure the lengths of the distal, middle and proximal phalanx. To find PROI, the ROI which contains all the phalanges and epiphyses, a number of steps are needed: First the lower boundary of the PROI is detected by scanning a horizontal line over the hand image to search for the soft tissue between the first index finger and the thumb. The upper boundary is a horizontal line at the tip of the third finger. After this two vertical lines are scanned from the middle of the hand to both the left and the right boundary of the hand. Each of the lines stop on the last pixel belonging to the hand, now the upper, lower, left and right boundary of the PROI have been defined. To segment the bones and epiphyses from the PROI it is first turned into a gradient image using two Sobel kernels. The result is thresholded using an empirically determined value to find the edges of the bones and epiphyses. The concentration of pixel values at the end of a phalanx is up to 50 percent higher than in the central part. Once a window has been determined that contains the epiphysis, a horizontal line is scanned over the window. The location of the smallest intersection with the segmented finger is marked as the line that separates the phalanges. In this fashion the borders between the third distal, middle and proximal phalanges are marked. These can now be measured. This method was tested on 50 pediatric hand CR (computed radiography) images and the results were compared to the measurements of an independent radiologist. The mean difference between these two measurements was 0.02mm with a mean standard error of 0.08mm. One year later this updated method was published by Pietka [23]. In this method the author attempts to determine the ratio between the width of the metaphysis and the width of the epiphysis. These measurements play a role in determining the stage of an EMROI. Finding the epiphysis and metaphysis happens in the same way as in Pietka [22]. After these two objects are found, their width is measured. The width is detected by calculating the derivative along a perpendicular line to the phalangeal axis. Maxima in this function indicate the borders of the epiphysis and metaphysis. The author reports that in a test with 80 hand CR images, accurate measurements of

the width of the metaphysis and epiphysis were found in 83 percent of the cases.

Efford [24] presents an analysis method that is driven, where possible, by knowledge of the hand/wrist anatomy. First the contour of the hand is segmented from the background manually. Regions of interest like the fingers are detected using curvature analysis of the contour of the segmented hand. Places in which the curvature is high mark the top of the fingers and the location of the inter-digital web. By fitting a polynomial through the inter-digital web locations (the inter-digital web is the piece of skin connecting two fingers at their base) each of the fingers can be isolated. When the fingers have been isolated the phalangeal axis of the finger is determined which can, when lengthened, give an indication of the location of the metacarpal centers. Using these metacarpal centers, the author test a number of deformable models to edge-detect the metacarpals. These include snakes, parametric Fourier models and active shape models. The author suggests using an expert system to automate skeletal age assessment, the written criteria found in the TW2 method should be translated into rules for the expert system. Measurements needed by the expert system could then be obtained directly from the parameters of the deformable models used in the segmentation. This system is not worked out in detail.

Manos [25] developed a segmentation method for the bones in the wrist using region growing and merging. The technique that is used is basically a bottom up approach. This means that the results of each stage of processing yield the data for the next. The method can be subdivided into several stages:

- Preprocessing stage
- Region growing stage
- Region merging stage
- Region merging by fusion of edge and region information
- Region labeling

In the preprocessing stage a Canny edge detector is used to find edges in the image. After these had been found the original image was smoothed with an edge-preserving smoothing filter. In the first region growing stage simple regions are formed by an algorithm that includes neighboring pixels in a region if their grey level difference is less than an empirically determined value. The resulting regions are then merged using a technique which is based on combining three merging scores representing region similarity, size and connectivity into a global merge score. The technique basically encourages regions with the same grey level characteristics to merge, larger regions are preferred over small ones while regions with little common boundary are discouraged to merge. The next stage involves comparing the edges found by the previous steps to region information from a separately edge-detected (from the preprocessing stage) image. Only the edges that are approximately the same in both images are kept. Only 15-20 percent of the edges that the first stage yielded are now left. The final stage involves the labeling of the remaining stages. Each region is labeled either they were 'bone' or 'background'. Labeling is performed through the application of a set of heuristic rules which are mainly based on the gray level characteristics of radiographs. Limited success in a test of 20 radiographs is reported by the author but no numerical data is presented.

Morris [26] presents an algorithm which uses domain knowledge in combination with a local statistical enhancement process. Because the difference in gray levels between bone and non-bone pixels is not consistent throughout the image simple threshold on the original image will not work. To alleviate this problem a statistical enhancement process is deployed. The most important result of this process is that the grey level of bone regions throughout the image becomes approximately the same. In the statistically enhanced image the five fingers are found by examining the peaks of a histogram taken over a horizontal line through the center of gravity of the hand. The five highest peaks represent the location of the four fingers and the thumb. Next domain knowledge of the anatomy of the hand is used to find the regions where the phalanges should approximately be. Once these regions have been found the edges of the phalanges in them are enhanced using a Sobel operator. To ensure a closed contour a line following algorithm is used on the edge enhanced phalanges. The author tested

the algorithm on six x-rays of hands of children in different age groups and shows a test on the radiograph of a young child.

Mahmoodi [27] describes a method to find the edges and location of the phalanges using Active Shape Models. To determine appropriate starting points for the ASM algorithm first the entire hand is segmented from the background. This is done using a valley seeking algorithm to determine an appropriate intensity threshold from the image histogram. Next the fingers are found by calculating the Euclidian distance between a point in the wrist and every point on the hand contour. This produces a hand contour signature in which the maxima represent the finger tips and the minima the finger bases. Using knowledge of the hand anatomy, seed points are determined for the phalanges in the fingers. The seed points are used to position ASM in the image and these find the contours of the phalanges. An algorithm for the identification of joint space and phalanx margin locations on hand radiographs is presented by Duryea [28]. This algorithm was not specifically designed for use in determining the skeletal age; instead it is focused on measuring the distances between the phalanges. Measuring this distance can help in the diagnosis of Rheumatoid arthritis. However, the ROI in the fingers are the same for both applications. The first step is the manual creation of a mask image marking the location of non anatomical structures like labels. All radiographs were manually turned so that the fingers were pointing to the right and the wrist was on the left side of the image. The algorithm employs a multiple resolution approach so for each radiograph a set of 4 lower resolution images were produced. First a rough outline of the hand is determined by an edge detection routine. Proceeding along the outline of the hand groups of pixels forming vertical lines are tested as potential fingertips. From these the five best candidates are selected. The finger locations are then found by moving in the negative x direction following the path of the largest signal starting at each fingertip. This produces an array of points along the finger; these are then fitted to a straight line using the least squares method. The gray value profile along this line shows three peaks which mark the space between the phalanges. The author claims a 100 percent success rate in identifying the digits (54 out of 54 images) and a 99 percent success rate in determining the joint space locations. However, a number of images were excluded from the test. These included images of

hands wearing rings or digits being touched by other objects in the image (e.g.: Label or collimator edge).

Vogelsang [29] presents an algorithm that can automatically find the ROI in a hand radiograph using Active Shape Models. First a Canny edge detector is used to detect the edges of the bones and of the hand. Using the detected edges of the bones starting positions for the ASM are determined. Each bone in the hand has a specific ASM specially trained to detect its shape. Next, these ASM determine the exact positions and shapes of the bones. Results are not presented in the article.

A method to extract the EMROI from a hand radiograph is presented by Pietka [30]. Before the actual extraction of the EMROI takes place, the hand radiograph is first preprocessed. The orientation of the image is corrected so that the hand is always in a standard position. Then the background is removed from the image so only the hand remains. The analysis starts by extraction of the phalangeal tip. Once the tips are found the phalangeal axis is determined by moving downwards through the middle of the phalanges (middle determined by distance to edges of phalanges to left and right). To smooth the resulting line a median filter is used and then a third-order polynomial is fitted to it. The derivative of the pixel values along the central axis can be analyzed and extreme values of the derivative indicate the locations of the EMROI. The author used 200 clinical hand radiographs in a test; in 4 percent of radiographs the phalangeal tip was not detected. The gap between the epiphysis and metaphysis was not detected in 4 percent of all cases (24 out of 588).

In 1991 Pietka [22] presents a simple method to determine the skeletal age using the length of several phalanges. First the phalanges are segmented using an edge detection algorithm. After this, the lengths of the distal, middle and proximal phalanges are measured. These lengths are looked up in the phalangeal bone length table by Garn [31]. The approximate skeletal age can be read from this table. The conclusion of the author is that the standard phalangeal length table can only be used to give a rough estimation of the skeletal age. The mean difference with the actual skeletal age is 1.5 years. One of the original authors of the TW2 method has also been

working on automatically assigning TW2 scores to bones in the hand.

Tanner [32] presents an automatic system for skeletal age assessment called CASAS. The system uses a high-resolution monochrome video camera which captures the radiographic hand images that are put on a specially adapted light box. The user sees a stage analysis template on the screen and has to try to fit a bone to the template using the zoom feature of the camera and by moving the radiograph. Each stage of each RUS-TW2 ROI has its own template. These templates don't influence the computer rating but are used for placing the ROI in a consistent orientation and position. The digital analysis is done by representing the changes in density from point to point in the part of the radiograph that is displayed by a Fourier transformation. A Fourier series of 64 degrees is fitted to each horizontal line of the shown radiograph, and there is 64 such lines one above the other vertically. The shown radiograph is represented by 64x64/4=1024 image coefficients, though most of the information is contained in a smaller (manageable) subset. The average of several reference images of a certain stage can be used to make an average stage image. Using the Fourier coefficients, a new image of a stage can be classified. This is done by comparing the coefficients of the image with the average coefficients characterizing each successive stage and choosing the stage with the minimal average deviation of coefficient values. The results presented by the author show that the CASAS system rates radiographs with a high repeatability and less then one percent reversal (reversal occurs when the analysis of the same patient later produces a lower skeletal age). However, several drawbacks are also noted by the author. The system is sensitive to ill-positioned hands and it prefers X-rays with superior definition. The program rejects between 5 percent and 10 percent of all ratings due to poor matching of the coefficients. A number of later studies further evaluated the program. A study by Albanese [33] indicates that assessment of a radiograph is still operator dependent because the operator has to decide to keep or reject a result supplied by the system. Misclassification was also at an unacceptable level for some bones like the radius and the ulna according to the author.

Tanner [34] also noted the high misclassification of the radius and ulna (15 percent were rejected). An evaluation study by Teunenbroek [35] concludes that although

the variability of the TW2 ratings produced by CASAS is low, the variability of the results when expressed in skeletal age seem considerable. They therefore recommend skipping the skeletal age conversion step and just use the TW2 maturity score.

Pietka [36] presents a classification algorithm that uses a fuzzy classifier to assign a bone age to the PROI (Phalangeal ROI) in the second, third and fourth finger. The features used by the classifier are automatically extracted from a hand radiograph. There are three types of features that are used in the analysis. The first feature is the length of the distal, middle and proximal phalanges. The second feature is the ratio between the diameters of the epiphysis and metaphysis. The third feature is the amount of fusion between the epi and metaphysis. A fuzzy classifier is then used. After defining a membership function, features are processed yielding a matrix which maps the features to a year of age within a predefined range. The grades of membership are defined as membership function values in the interval 0-1. A classification rule based on a max-sum operator is used to process the matrix assessing the skeletal age. The results presented by the author show that a correct extraction of epiphyseal diameter / metaphyseal diameter ratios and phalangeal length has been obtained in 90 percent of all 1080 test cases.

In the later stages of skeletal development the size and shape of the epiphysis becomes less important. The amount of fusion between the epiphysis and metaphysis becomes the more important measure of skeletal age. In order to evaluate the amount of fusion Pietka [37] introduces the idea of using a wavelet decomposition analysis as a quantitative measure to estimate the amount of fusion. Four levels of fusion are distinguished: no fusion, early fusion, advanced fusion and fusion completed. The author claims a successful rating of the fusion in 83 percent of all 90 test cases. Evaluation of the actual amount of fusion has been done by visual inspection. The method is sensitive to under and overexposure of radiographs, if these are thrown out in a preprocessing step the accuracy of the analysis increases to 90 percent. In [17] Gross presents the results of a study that indicate simple neural networks could assist radiologists in the assessment of skeletal age. A database of 521 hand radiographs and a total of four features that were calculated from seven measurements were used to train the network.

The measurements included the widths of several epiphyses of the proximal phalanx and the lengths of those phalanxes. Also the length of the second metacarpal was included. The parameters were then derived from 4 ratios between several of the linear measurements. All measurements were obtained by hand. The parameters were used to train the neural network. The author claims that the results produced by the neural network can be compared with those of an experienced radiologist who uses a standard pediatric skeletal atlas (Greulich and Pyle [16]). Marques da Silva [38] presents a method to determine a digital signature for skeletal maturity. The end goal of the presented research is to determine a signature of the physiological process of skeletal maturity in terms of events that can be used to objectively assess bone age. The first step in the method determines the longitudinal axis of the middle finger (LAMF). A scale space technique is used to find the LAMF. When the image is viewed at an appropriate scale the LAMF is visible as a ridge in the image intensity landscape. In the next step the intensity transitions along the LAMF are examined using a gradient operator at a certain scale. The author claims that this can show the presence of the epiphysis and in the later TW2 stages the amount of fusion between epi and metaphysis. By using the distance between the peaks and valleys in the intensity profile the gaps between the phalanges and the lengths of the phalanges can be measured. The author uses the ratio between the length of the proximal phalanx and the length of the gap between this phalanx and the metacarpal as an indicator of skeletal maturity. Some preliminary results are presented.

3.1.3 Discussion

Much of the studies that have been done into finding the EMROI in the hand has focused on smart threshold techniques (e.g.: Micheals [21], Mahmoudi [27], Pietka [22] and Morris [26]) to find the outline of the hand. Once the outline has been found a variety of techniques can be used to find the EMROI. However, this threshold step is not trivial and some researchers skip it altogether and revert to a manual threshold operation such as Efford [24]. The problem with using a thresholding operating on a radiograph is that it is almost never successful for the entire radiograph. Heel effect

causes a gradient over the entire radiograph. The effect itself is caused by the fact that not all X-rays emitted from the X-ray tube are perpendicular to the target. The non perpendicular X-rays must travel a larger distance through the target (see Farr [39] and Behiels [40]). Because of this the grey value for a certain substance like bone or flesh is not constant over the entire radiograph. This makes segmentation using threshold very difficult and less robust.

Another approach is to detect the fingertips of the hand and use these as starting points for the segmentation of the fingers and the phalanges (Duryea [28] and Pietka [30]). Although both authors report excellent results one still is more or less dependent on a well defined border both left and right of the phalanges or finger in order to be able to segment it. Also these methods can be sensitive to disturbances in the background of the radiograph like labels or markers.

The advantage of using some type of deformable model and ASM in particular is that it is less sensitive to local disturbances in the contour of the object. It manages to segment an object even when part of the contour is not well defined because the model "knows" the shape of an object from a training set. Some research has been done using these types of models (e.g.: Mahmoudi [27], Vogels [29] and Efford [24]). Extensive evaluations have not been performed but indications are positive. The research into actually assigning a certain skeletal development stage or score to an EMROI can be subdivided into two approaches. One approach is to find measurements, for example the width or length of certain bones, and relate these measurements to a certain skeletal age. Then one can train a classifier and use it to assign the measurements of new cases to a certain skeletal age or TW2 score (e.g.: Pietka [22] [36] and Gross [17]). A disadvantage of this method is that at a certain point in the skeletal development, structures like epiphyses tend to gradually disappear because they fuse with the metaphysis. Epiphyses are often used in these measurement based techniques because their width supplies a lot of information about the skeletal development (until fusion starts). So most of these methods only yield accurate results until fusion starts.

Another approach is to use some kind of similarity measure for the general

appearance of an EMROI. And use this measure to compare a new instance of an EMROI with a set of averages of each TW2 or skeletal development stage. Tanner [32] demonstrated this with their CASAS system which represents the changes in density from point to point of the part of the radiograph containing the EMROI by a Fourier transformation in two dimensions. Of each TW2 stage the average representation is known. Tanner uses these average representations to compare with new images of EMROI. The results of this system presented by the author are good, but evaluation studies showed some problems. The largest problem with the CASAS system was that a human operator was still involved in the process. This operator had to align each EMROI with a template and if this was not done correctly it had a large impact on the quality of the classification. Because of the precise alignment the analysis still took a lot of time and the operator still needed to know the TW2 system well enough to recognize wrong classifications by the system.

4. MATERIALS AND METHODS

4.1 Bone Age Assessment Methodology Overview Of Carpal ROI Analysis

The work flow of carpal ROI analysis procedure which includes seven steps is shown in Figure 4.1. The carpal bone region of interest was first extracted from the entire hand image (1). Due to the non-uniform background and noise, the carpal bone ROI was subjected to an anisotropic diffusion filter (2) which smoothed out the noise and preserves the edges at the same time. Then, the object contours were extracted by the canny edge detector (3). A series of operations based on morphological properties of segmented objects were implemented in order to single out the carpal bones by eliminating the non-carpal bones (4). The carpal bones contours went through feature extraction phase which yields the inputs into the neural network classification to assess the bone age (5). This section discusses the procedure in the following order: carpal bone segmentation, carpal bone identification, feature analysis and bone age assessment using neural network.

4.2 Carpal Bone Segmentation

4.2.1 Carpal ROI Extraction From Entire Hand Image

The first step in Figure 4.1 was to locate and extract carpal ROI for further analysis. The upper edge of the carpal ROI was defined by a horizontal line and searching for the junction between the second and third metacarpal bone. The lower edge of the CROI was the line that intersected the forearm with the minimal width. The carpal ROI was defined within these four edges by using the imcrop function tool which is defined in MATLAB7 software program. An example of the extracted carpal ROI is illustrated in Figure 4.3.

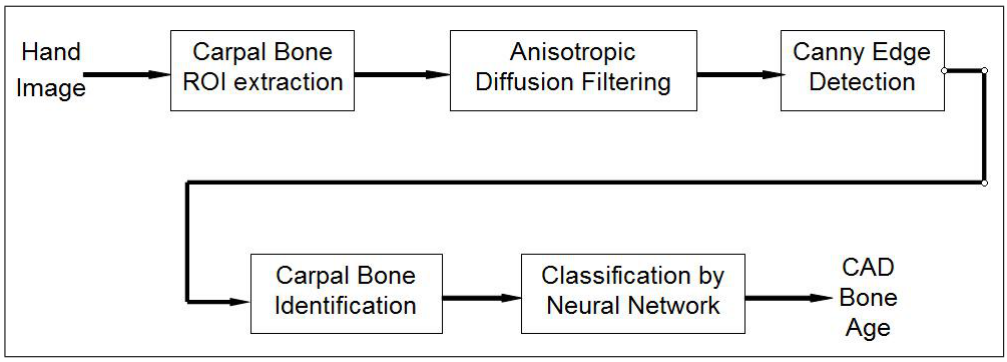

Figure 4.1 Carpal ROI analysis workflow with 5 steps

Figure 4.2 Left hand x-ray image

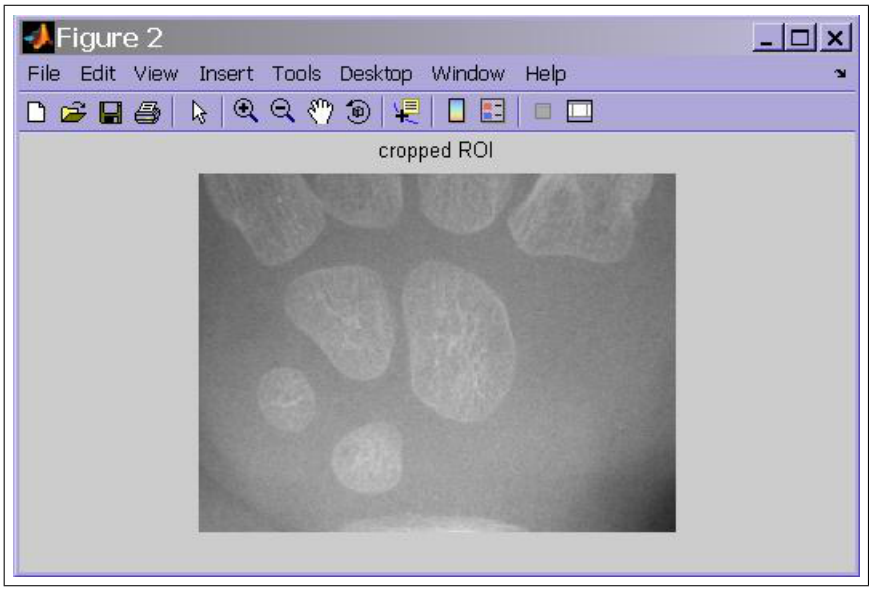

Figure 4.3 Cropped Carpal Region of Interest

4.2.2 Image Smoothing By Anisotropic Diffusion

Carpal bones in the image are generally poor in contrast. Furthermore, the bone edges are often degraded by noise and artifacts. In order to better differentiate carpal bones from the background, an anisotropic diffusion filter proposed by Perona and Malik [41] was applied to the carpal ROI image which is the second step in Figure 4.1. This filter was able to greatly reduce noise in homogeneous areas of carpal ROI images while preserving the edges and contrast associated with bony structures.

The principle is to smooth out noise locally by diffusion while at the same time preventing diffusion across object boundaries. The diffusion coefficient is chosen to vary spatially based on a measure of edge strength to encourage intra-region smoothing in preference to inter-region smoothing. The diffusion process achieves piecewise smoothing while preserving the relevant image edges. Thus, the noise is greatly suppressed by the diffusion process while the sharp edges are well preserved. Also, the parameters for the anisotropic filter is illustrated in Figure 4.4.

Size and shape of carpal bone are the characteristics related with skeletal development. Bony texture inside the carpal bone is not the factor that radiologist

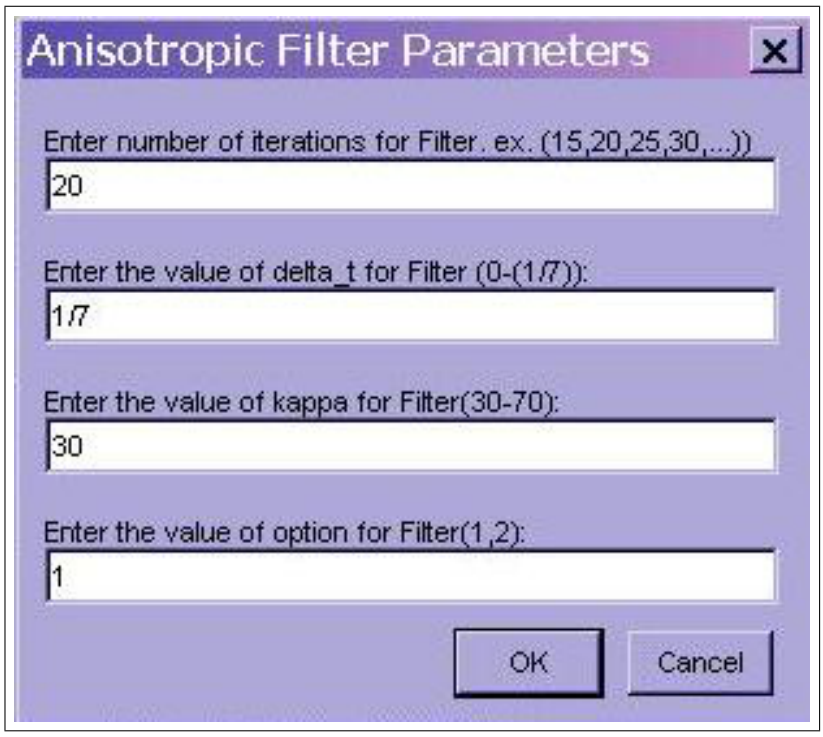

Figure 4.4 Anisotropic Filter Parameters

investigate in assessing the bone age. The next step is to segment the carpal bones from the carpal ROI image.

4.2.3 Edge Detection By Canny

Edge detection by Canny method third step in Figure 4.1 was performed on the smoothed ROI image. The Canny edge detector finds linear, continuous edges and is known as the optimal edge detector [5] [42] [43]. The Canny method differs from other edge detection methods in that it uses two different thresholds, and includes the weak edges in the output only if they are connected to strong edges. So, the image is filtered by using the anisotropic diffusion and the edges are detected by Canny method. This method is less likely than the others to be confused by noise and the carpal bones were detected as closed-contours.

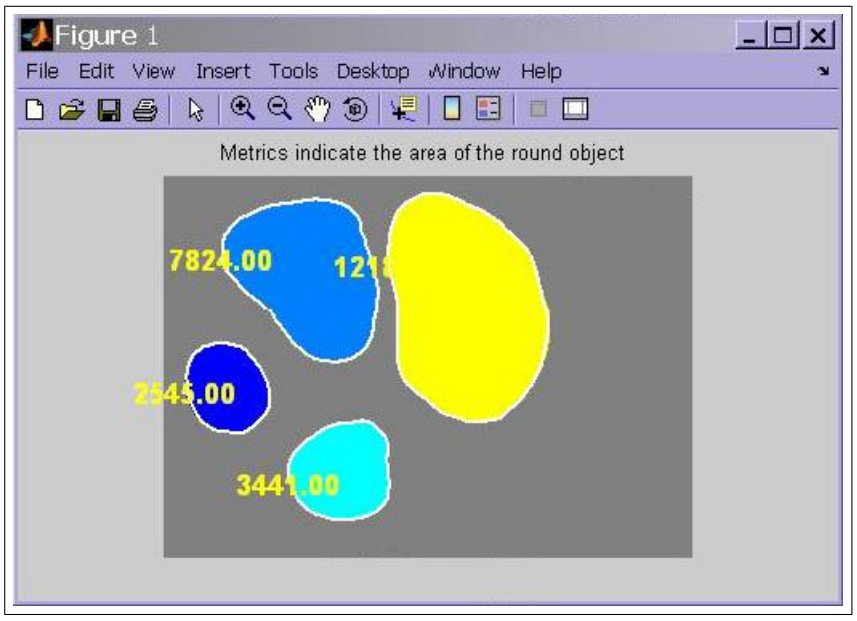

Figure 4.5 Areas of four of the Carpal Bones

4.2.4 Carpal Bone Identification

In this part, our goal is to classify objects based on their roundness using bwboundaries, a boundary tracing routine. First of all, we read the images by imread function. Secondly, threshold is applied to the images to convert the image to black and white in order to prepare for boundary tracing using bwboundaries. In the third step of carpal bone identification, noise is removed. Using morphology functions, the pixels which do not belong to the objects of interest are removed. All objects containing fewer than 90 pixels are removed, the probable gaps and holes are filled so that regionprops can be used to estimate the area enclosed by each of the boundaries. In step 4, we found the boundaries of the carpal bones as shown in Figure 4.5. In this stage we concentrate only on the exterior boundaries. The option 'noholes' that we used accelerates the processing by preventing bwboundaries from searching for inner contours. Finally, the area of the each object in carpal region of interest is calculated. Regionprops is used to obtain estimates of the area for all of the objects. Notice that the label matrix returned by bwboundaries is reused by regionprops.

The area of object which is not detected by the automated system can be calcu-

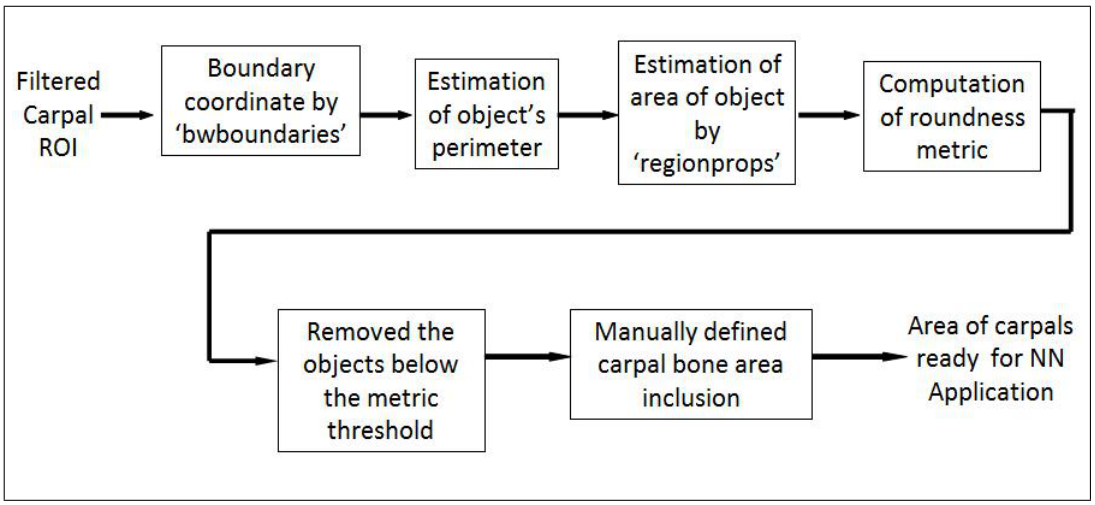

Figure 4.6 Carpal Bone Feature Extraction Steps

lated by the operator. In that case, operator chooses the points on the boundaries of the carpal bones. These points are interpreted as the X and Y coordinates and another part of the code calculates the area of this region. Also, all these calculated areas are plotted on the GUI of the MATLAB7 software program. Steps illustrated in Figure 4.6.

4.2.5 Bone Age Assessment With Neural Network Application

In this stage, the areas of the carpal bones are directed to the neural network via the GUI seen in Figure 4.6 as inputs of the neural network. The chronological age is given to the neural network as the target to be converged. Furthermore, the neural network is created with 1 hidden layer and 1 output layer. Additionally, the hidden layer might consist of 3,5,15,75 neurons depending on the convergence performance of the neural network in our study. For both male and female categories, networks are trained with levenberg-marquardt training algorithm. In the evaluation stage, some test images are given to the trained neural network as inputs as seen in Figure 4.7. Then, we have taken the outputs from neural network as our test image age. After this stage, standard deviation is calculated for both male and female category.

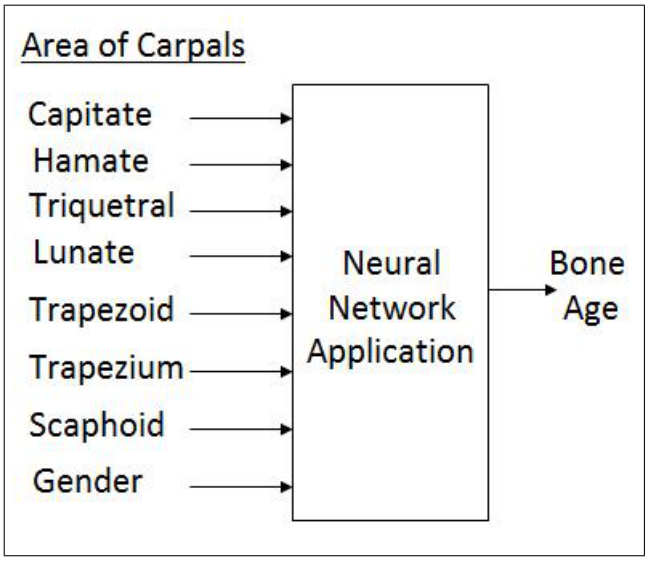

Figure 4.7 Neural Network Application

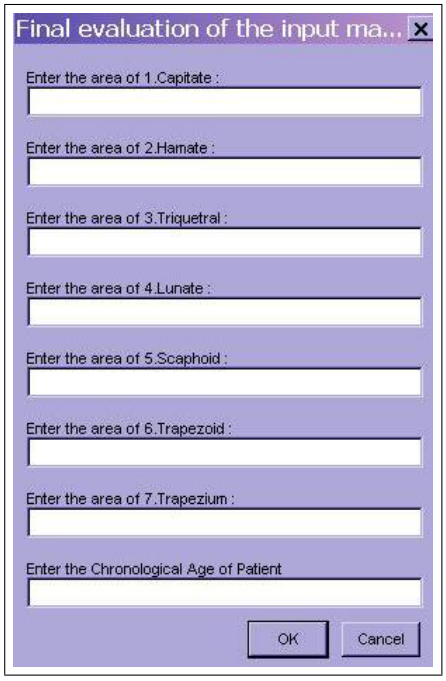

Figure 4.8 Carpal Bone Areas are entered to the Neural Network

5. Results

In this study, hand Xray images for females of age groups from 0 to 5 and males from 0 to 7 from the collection of 294 images went through the carpal ROI analysis. The work also consisted of carpal bone segmentation, feature extraction and neural network training for the computer aided bone age assessment. The results of CAD bone age are presented in this chapter.

The CAD results in all the tables and figures are based on the carpal ROI which were compared with the reading of two radiologists. CAD results are obtained after the neural network is created out of 236 training Xray images. Tests are completed with total of 58 Xray images.

Firstly, to give an idea of the performance of each feature in assessing the bone age, correlation with the chronological age is demonstrated in Table 5.1. These correlation coefficients are calculated based on the size feature of the carpal bones.

In Table 5.2, Table 5.3 and Table 5.4, mean differences of the two radiologist readings and the CAD bone ages are illustrated. In the mentioned tables, test 1 stands for one of the eight categories which is Hispanic race and female gender. In test 2, there are two categories as male and female. Lastly, in test 3 one universal category exists.

In Figure 5.1, all seven carpal bones went through the process for test 1, test 2 and test 3. In Figure 5.2, capitate and hamate bones are excluded from the calculations. In this way, another approach is shown for the overlapped bone cases because it is seen that capitate and hamate overlaps in some cases. Also, trapezoid and trapezium overlaps in some cases. Thus, in Figure 5.3, other calculations are illustrated after trapezoid and trapezium bones are excluded.

Table 5.1
Correlation coefficients between size of carpals and chronological age

	Cap.	Ham.	Triq.	Lun.	Trapezoid	Trapezium	Scap.
Correlation Coefficient	0,94	0,90	0,88	0,85	0,72	0,76	0,73

Table 5.2
Correlation coefficients between size of carpals

	1	2	3	4	5	6	7
1	1						
2	0,93	1					
3	0,89	0,89	1				
4	0,84	0,85	0,89	1			
5	0,74	0,77	0,83	0,81	1		
6	0,77	0,81	0,89	0,90	0,82	1	
7	0,75	0,76	0,84	0,84	0,90	0,85	1

Table 5.3
All Carpals Mean Difference Table

	Test1	Test2		Test3
		Male	Female	
Reading 1	-0,25	0,22	0,21	0,18
Reading 2	-0,05	0,13	0,23	0,13
CAD BA	0,54	-0,12	-0,06	0,08

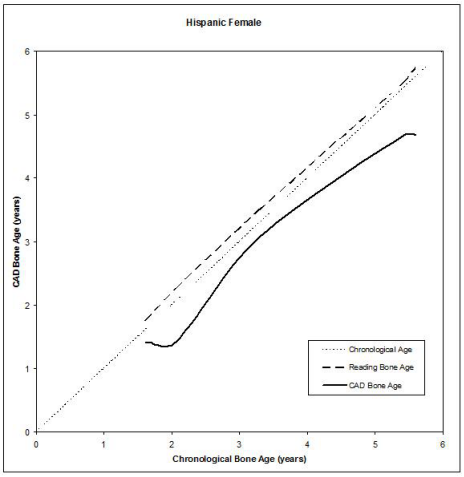

(a) Hispanic Female

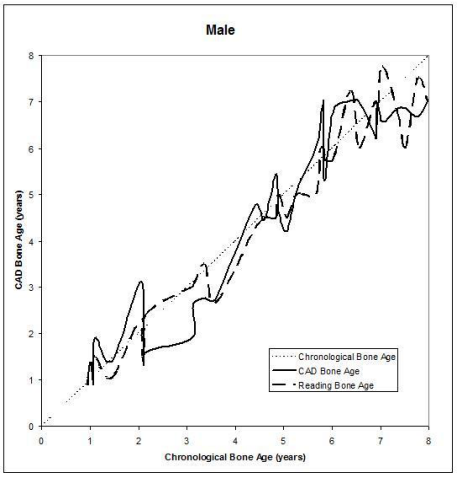

(b) Male Gender With All Races

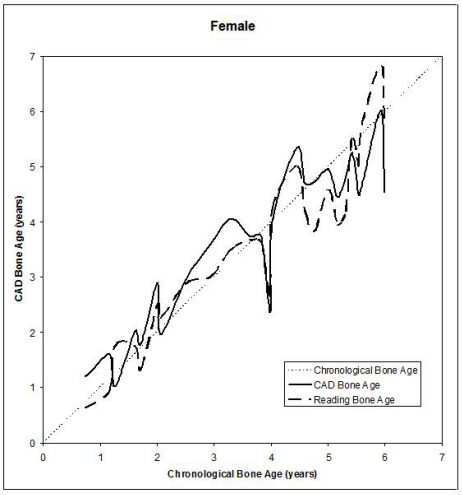

(c) Female Gender With All Races

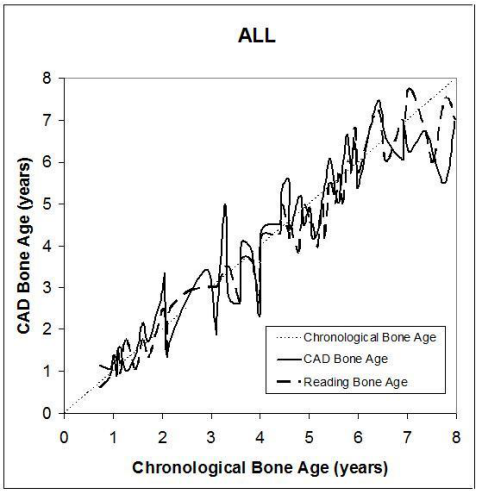

(d) All Genders and Races

Figure 5.1 (a), (b), (c) and (d) illustrates the results for Test1, Test2 and Test3 with all the carpal bones included

Table 5.4
Capitate and Hamate Excluded: Mean Difference Table

	Test1	Test2		Test3
		Male	Female	
Reading 1	-0,25	0,22	0,21	0,18
Reading 2	-0,05	0,13	0,23	0,13
CAD BA	-0,06	-0,09	-0,03	0,19

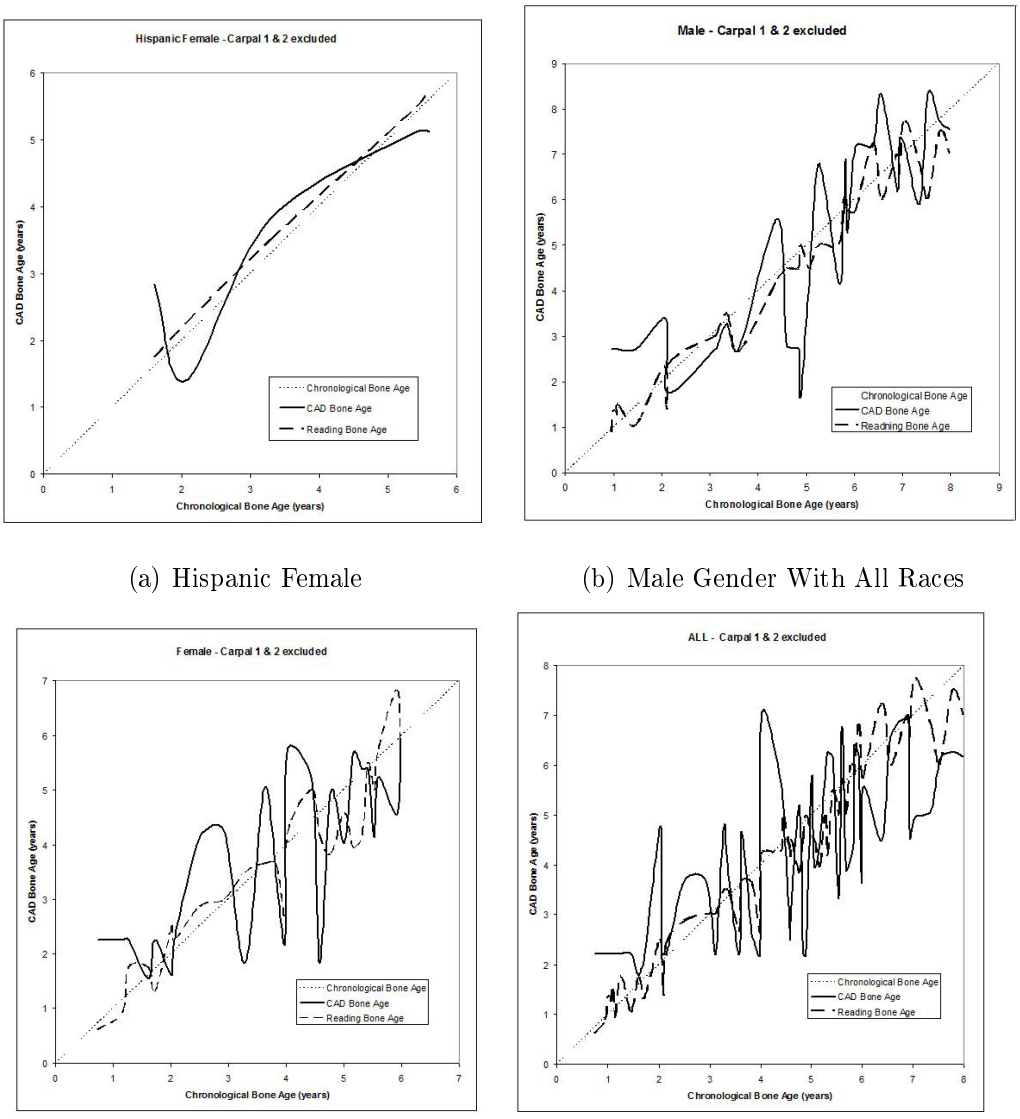

(a) Hispanic Female

(b) Male Gender With All Races

(c) Female Gender With All Races

(d) All Genders and Races

Figure 5.2 (a), (b), (c) and (d) illustrates the results for Test1, Test2 and Test3 with Capitate and Hamate excluded

Table 5.5
Trapezoid and Trapezium Excluded Mean Difference Table

	Test1	Test2		Test3
		Male	Female	
Reading 1	-0,25	0,22	0,21	0,18
Reading 2	-0,05	0,13	0,23	0,13
CAD BA	0,20	0,20	0,00	0,06

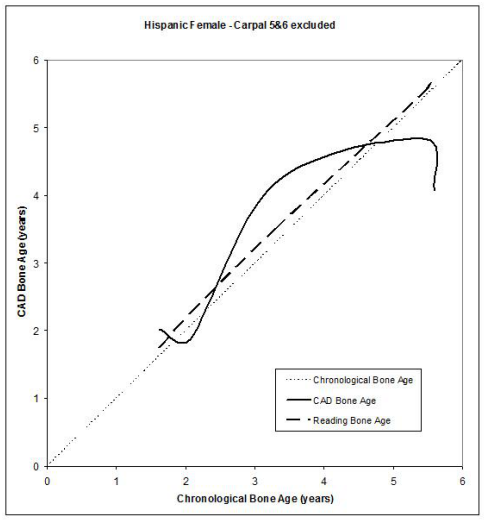

(a) Hispanic Female

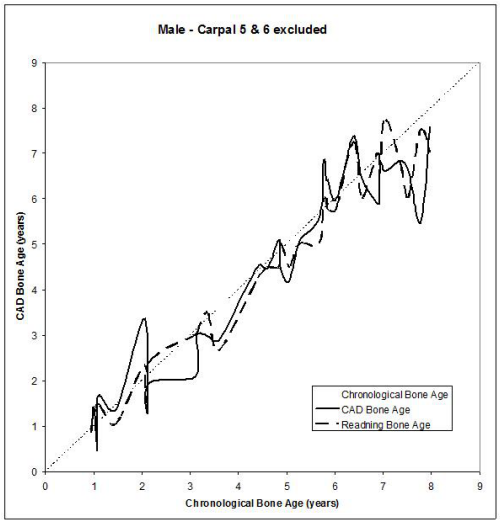

(b) Male Gender With All Races

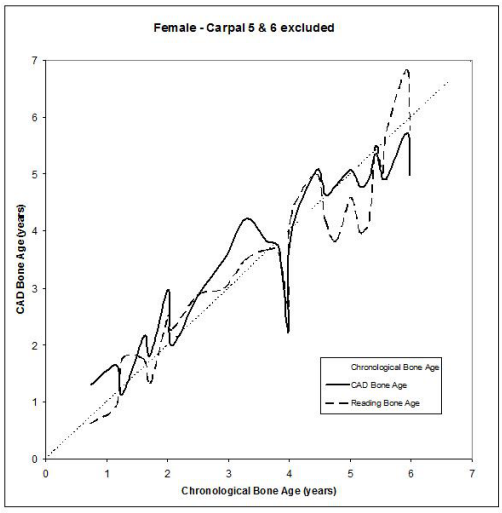

(c) Female Gender With All Races

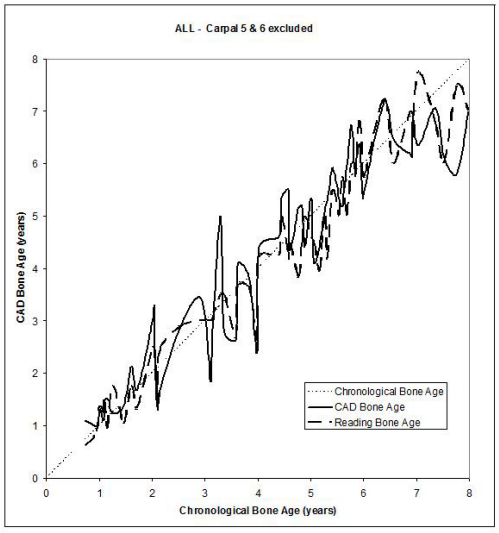

(d) All Genders and Races

Figure 5.3 (a), (b), (c) and (d) illustrates the results for Test1, Test2 and Test3 with Trapezoid and Trapezium excluded

6. Conclusion

A method based on the determination of the seven carpal bones is applied in this study. The method consists of carpal bone segmentation, carpal ROI extraction, image smoothing, edge detection, carpal bone identification, neural network application. The developed software program is tested on total of 58 Xray images. As different race and gender shows diverse growth patterns, we have studied on a single race and gender which is hispanic and female, also for the comparison in test 2 all the races are combined and finally in test 3 a universal category is created.

The computerized bone age assessment results which are obtained by neural network are evaluated by comparison with the chronological age of Xray images. Based on correlation coefficient, mean difference tables and figures illustrated in results chapter, it is verified that feature extraction of carpal ROI is a good indicator for bone age assessment of young children.

Additionally, it is important to be mentioned that carpal ROI has some advantages over phalangeal ROI for young children. In phalangeal ROI evaluation, finger bend and hand rotation during acquisition is important. However, for carpal ROI evaluation, this does not make much difference. Also, earlier studies in the literature illustrates us that for ages below 5-7, the phalangeal analysis fails to extract the features correctly. This is due to the following problems: first, soft tissue deteriorates the border and makes the segmentation between epiphysis and metaphysis an extremely difficult task. Second, the developments of epiphysis of the six phalangeal ROIs are not parallel. Third, it is not reliable to locate the phalangeal ROIs correctly if the hand is rotated when the upright hand position is not achieved during acquisition. Lastly, the phalangeal ROIs analysis is sensitive to bending of fingers during acquisition[17].

Moreover, in tables which displays mean differences, it show us that two radiologist might have different evaluations even if they use the same matching atlas which

is Greulich and Pyle atlas in this case. In case of using different evaluation techniques by radiologists, the inter-observer discrepancy might sometimes become larger. Because of that reason, computerized studies such as this one and many others could provide radiologists another opinion and help through evaluation process to improve the accuracy in clinical practice.

6.1 Future Work

In this study, the further development of the computer-aided-diagnosis bone age assessment method could be expected. It can be improved in several ways. First, by including other features of carpal bone like eccentricity and triangularity in evaluation process might be worthwhile to improve the accuracy of the method. Moreover, semi-automatic parts of the software could be improved to a full-automatic system. Secondly, this study could be extended to all age groups of people until 18 years old. Also, a user friendly GUI application could be really helpful for radiologists in order to benefit from the CAD bone age assessment system. Additionally, using atlas reference images as the source and training purposes might be another approach. That approach might help us to have a 3 month precision. When we compare that with our current work, it is a long time. However, 3 month precision is what pediatricians expect as a result. A CAD system with the improvements mentioned above would be implemented in radiology department of hospitals.

APPENDIX A. MATLAB FILES OF BAA SOFTWARE

main.m

Main file of the software which helps for the flow of the code

segmentate.m

Used for segmentation of the X-ray images

enterarea.m

Enables to enter the areas of the round object to matrices

interpolate.m

Joins the manually marked object boundaries

closedarea.m

Calculates the area of the round object

anisodiff.m

Applies the anisotropic diffusion filter for two dimensional Xray images

REFERENCES

1. Gertych, A., A. Zhang, J. Sayre, S. Pospiech-Kurkowskac, and H. K. Huang, "Bone age assessment of children using a digital hand atlas," *Computerized Medical Imaging and Graphics*, p. 322, 2007.

2. Greulich, W. W., and S. I. Pyle", *Radiographic atlas of skeletal development of hand wrist. 2nd ed.*, Stanford, California: Stanford University Press, 1971.

3. Gilsanz, V., and O. Ratib, *Hand Bone Age: A Digital Atlas of Skeletal Maturity*, Verlag Berlin Heidelberg, 2005. p.2.

4. Greulich, W. W., and S. I. Pyle, *Radiographic atlas of skeletal development of handwrist*, California: Stanford University Press, 1959.

5. Zhang, A., A. Gertych, B. Liu, H. K. Huang, and S. Pospiech, "Carpal bone segmentation and features analysis in bone age assessment of children," *Proceedings of the RSNA conference*, p. 688, 2005.

6. Johnston, F. E., and S. B. Jahina, "The contribution of the carpal bones to the assessment of skeletal age," *Journal of Physics*, Vol. 23, pp. 349–354, 1965.

7. Lowrey, G. H., *Growth and Development of Children. 8th ed.*, Chicago: Medical Publishers, Inc., 1986.

8. Kuhns, L. R., and O. Finnstrom, "New standards of ossification of the newborn," *Radiology*, Vol. 119, pp. 655–660, 1976.

9. Keats, T. E., *The Bones: Normal and Variants*, Philadelphia: Caffey's Pediatric Diagnostic Imaging, 10th ed., 2004.

10. Morishima, A., M. M. Gumbach, E. R. Simpson, C. Fisher, and K. Qin, "Aromatase deficieny in male and female siblings caused by a novel mutation and the physiological role of estrogens," *Journal of Clinical Endocrinology*, Vol. 80, pp. 3689–3698, 1995.

11. Kaplan, S. A., *Growth and Growth Hormone: Disorders of the anterior pituitary*, Philadelphia: W. B. Saunders Company, 2nd ed., 1990.

12. Tanner, J. M., R. H. Whitehouse, and W. A. Marshall, *Assessment of Skeletal Maturity and Prediction of Adult Height by TW2 Method*, New York: Academic Press, 1975.

13. Roch, A. F., G. H. Davila, and S. L. Eyman, "A comparison between greulich-pyle and tanner-whitehouse assessments of skeletal maturity," *Radiology*, Vol. 98, p. 273, 1971.

14. Tanner, J. M., and R. D. Gibbons, "A computerized image analysis system for estimating tanner-whitehouse 2 bone age," *Hormone Research*, Vol. 42, no. 6, pp. 282–287, 1994.

15. Pietka, E., S. Pospiech, A. Gertych, F. Cao, H. K. Huang, and V. Gilsanz, "Computer automated approach to the extraction of epiphyseal regions in hand radiographs," *Journal of Digital Imaging*, Vol. 14, pp. 165–172, 2001.

16. Greulich, W. W., and S. I. Pyle, *Radiographic Atlas of Skeletal Development of Hand and Wrist*, Stanford University Press, 2nd ed., 1971.

17. Zhang, A., A. Gertych, and B. Liu, "Automatic bone age assessment for young children from newborn to 7-year-old using carpal bones," *Computerized Medical Imaging and Graphics*, Vol. 31, pp. 299–310, 2007.

18. Hsieh, C. W., T. L. Jong, and C. M. Tiu, "Bone age estimation based on phalanx information with fuzzy constrain of carpals," *International Federation for Medical and Biological Engineering*, Vol. 45, no. 3, pp. 283–295, 2007.

19. Pietka, E., L. Kaabi, M. L. Kuo, and H. K. Huang, "Feature extraction in carpal-bone analysis," *IEEE Transactions on medical Imaging*, Vol. 12, no. 1, pp. 44–49, 1993.

20. Liu, J., J. Qi, Z. Liu, Q. Ning, and X. Luo, "Automatic bone age assessment based on intelligent algorithms and comparison with tw3 method," *Computerized Medical Imaging and Graphics*, Vol. 32, pp. 678–684, 2008.

21. Michael, D. J., and A. C. Nelson, "Handx: a model-based system for automatic segmentation of bones from digital hand radiographs," *IEEE Transactions on Medical Imaging*, Vol. 8, no. 1, pp. 64–69, 1989.

22. Pietka, E., M. F. McNitt-Gray, M. L. Kuo, and H. K. Huang, "Computerized bone analysis of hand radiographs," *IEEE Transactions on Medical Imaging*, Vol. 10, pp. 616–620, 1991.

23. Pietka, E., M. F. McNitt-Gray, T. Hall, and H. K. Huang, "Computerized bone analysis of hand radiographs," *SPIE Medical Imaging*, Vol. 1652, pp. 522–528, 1992.

24. Efford, N. D., "Knowledge-based segmentation and feature analysis of handwrist radiographs," technical report, University of Leeds, 1994.

25. Manos, G. K., A. Y. Cairns, I. W. Rickets, and D. Sinclair, "Segmenting radiographs of the hand and wrist," *Computer Methods and Programs in Biomedicine*, Vol. 43, pp. 227–237, 1994.

26. Morris, D. T., and C. F. Walshaw, "Segmentation of the finger bones as a prerequisite for the determination of bone age," *Image and Vision Computing*, Vol. 12, no. 4, pp. 239–246, 1994.

27. Mahmoodi, S., B. S. Sharif, E. G. Chester, J. P. Owen, and R. E. J. Lee, "Automated vision system for skeletal age assessment using knowledge based techniques," *IEEE conference publication*, Vol. 443, pp. 809–813, 1997.

28. Duryea, J., Y. Jiang, P. Countryman, and H. K. Genant, "Automated algorithm for the identification of joint space and phalanx margin locations on digitized hand radiographs," *Medical Physics*, Vol. 26, no. 3, pp. 453–461, 1998.

29. Vogelsang, F., M. Kohnen, H. Schneider, F. Weiler, M. W. Kilbinger, B. B. Wein, and R. W. Gunter, "Skeletal maturity determination from hand radiograph by model based analysis," *Proceedings SPIE*, Vol. 3979, pp. 294–305, 2000.

30. Pietka, E., A. Gertych, S. Pospiech, F. Cao, H. K. Huang, and V. Gilsanz, "Computer-assisted bone age assessment: Image preprocessing and epiphyseal-metaphyseal roi extraction," *IEEE Transaction on Medical Imaging*, Vol. 20, no. 8, pp. 715–729, 2001.

31. Garn, S. M., K. P. Herzog, A. K. Poznanski, and J. M. Nagy, "Metacarpophalangeal length in the evaluation of skeletal malformation," *Radiology*, Vol. 105, pp. 375–381, 1972.

32. Tanner, J. M., and R. D. Gibbons, "A computerized image analysis system for estimating tanner-whitehouse 2 bone age," *Hormone Research*, Vol. 42, no. 6, pp. 282–287, 1994.

33. Albanese, A., C. Hall, and R. Stanhope, "The use of a computerized method of bone age assessment in clinical practice," *Hormone Research*, Vol. 44, no. 3, pp. 2–7, 1995.

34. Tanner, J. M., D. Oshman, G. Lindgren, J. A. Grunbaum, R. Elsouki, and D. Labarthe, "Reliability and validity of computer-assisted estimates of tanner-whitehouse skeletal maturity (casas): comparison with the manual method," *Hormone Research*, Vol. 42, pp. 288–294, 1994.

35. van Teunenbroek, A., W. de Waal, A. Roks, P. Chinafo, M. Fokker, P. Mulder, S. de Muinck Keizer-Schrama, and S. Drop, "Computer-aided skeletal age scores in healthy children, girls with turner syndrome, and in children with constitutionally tall stature," *Pediatric research*, Vol. 39, no. 2, pp. 360–369, 1996.

36. Pietka, E., "Computer-assisted bone age assessment based on features automatically extracted from a hand radiograph," *Computerized Medical Imaging and Graphics*, Vol. 19, no. 3, pp. 251–259, 1995.

37. Pietka, E., and H. K. Huang, "Epiphyseal fusion assessment based on wavelets decomposition analysis," *Computerized Medical Imaging and Graphics*, Vol. 19, no. 6, pp. 465–472, 1995.

38. da Silva, A. M. M., S. D. Olabarriaga, C. A. Dietrich, and A. A. Schmitz, "Initial steps towards a digital signature for skeletal maturity," technical report, 2001.

39. Farr, R. F., and P. J. Allisy-Roberts, *Physics for Medical Imaging*, London: W B Saunders Company Ltd, 1997. 1st edition.

40. Behiels, G., F. Maes, D. Vandermeulen, and P. Sueten, "Retrospective correction of the heel effect in hand radiographs," *Medical Image Computing and Computer-Assisted Intervention*, pp. 301–308, 2001.

41. Perona, P., and J. Malik, "Scale-space and edge detection using anisotropic diffusion," *PAMI*, Vol. 12, no. 7, p. 629, 1990.

42. Canny, J. F., "Finding edges and lines in images," Master's thesis, Massachusetts Institute of Technology, 1983.

43. Canny, J. F., "A computational approach to edge detection," *IEEE Trans PAMI*, Vol. 8, no. 6, p. 679, 1986.